Low Incidence of Off-Target Mutations in Individual CRISPR-Cas9 and TALEN Targeted Human Stem Cell Clones Detected by Whole-Genome Sequencing

Low incidence of off-target mutations in individual CRISPR-Cas9 and TALEN targeted human stem cell clones detected by whole-genome sequencing

Adrian Veres[1,2], Bridget S. Gosis[1], Qiurong Ding[1], Ryan Collins[3], Ashok Ragavendran[3], Harrison Brand[3], Serkan Erdin[3], Chad A. Cowan[1,2,5], Michael E. Talkowski[3,4,5] & Kiran Musunuru[1,2,5,6]

1. Department of Stem Cell and Regenerative Biology, Harvard University, and Harvard Stem Cell Institute, Cambridge, Massachusetts 02138, USA

2. Department of Medicine, Harvard Medical School, Boston, MA 02115, USA

3. Molecular Neurogenetics Unit, Psychiatric and Neurodevelopmental Genetics Unit, Center for Human Genetic Research, Massachusetts General Hospital, Boston, MA 02114, USA

4. Department of Neurology, Harvard Medical School, Boston, MA 02115, USA

5. Broad Institute, Cambridge, Massachusetts 02142, USA

6. Division of Cardiovascular Medicine, Brigham and Women's Hospital, Boston, MA 02115, USA

Corresponding Author

Kiran Musunuru, M.D., Ph.D., M.P.H.

Harvard University

Sherman Fairchild Biochemistry Bldg 160

7 Divinity Ave

Cambridge, MA 02138, USA

E-mail: kiranmusunuru@gmail.com / Phone: (617) 496-5361 / Fax (617) 496-8351

Running Title: Whole-genome sequencing of genome-edited clones

SUMMARY

Genome editing has attracted wide interest for the generation of cellular models of disease using human pluripotent stem cells and other cell types. CRISPR-Cas systems and TALENs can target desired genomic sites with high efficiency in human cells, but recent publications have led to concern about the extent to which these tools may cause off-target mutagenic effects that could potentially confound disease-modeling studies. Using CRISPR-Cas9 and TALEN targeted human pluripotent stem cell clones, we performed whole-genome sequencing at high coverage to assess the degree of mutagenesis across the entire genome. In both types of clones, we found that off-target mutations attributable to the nucleases were very rare. From this analysis, we suggest that while some cell types may be at risk for off-target mutations, the incidence of such effects in human pluripotent stem cells may be sufficiently low to not be a significant concern for disease modeling and other applications.

Clustered regularly interspaced short palindromic repeats (CRISPR)-CRISPR-associated (Cas) systems and transcription activator-like effector nucleases (TALENs) are recently developed genome-editing tools that target desired genomic sites in mammalian cells (Miller et al., 2011; Hockemeyer et al., 2011; Cong et al., 2013; Mali et al., 2013b; Cho et al., 2013; Jinek et al., 2013). The most commonly employed CRISPR-Cas system, derived from *Streptococcus pyogenes*, uses Cas9 nuclease that complexes with a guide RNA that hybridizes a 20-nucleotide DNA sequence (protospacer) immediately preceding an NGG motif (protospacer-associated motif, or PAM), resulting in a double-strand break (DSB) three basepairs (bp) upstream of the NGG (Jinek et al., 2012). TALENs bind as a pair on sequences surrounding a genomic site, positioning a dimer of FokI nuclease domains to generate a DSB at the site. The introduction of a DSB at a specified genomic site allows for modification of the site via either non-homologous end joining (NHEJ), which typically introduces an insertion or deletion (indel), or homology-

directed repair (HDR), which can be exploited to knock in a point mutation or insert a desired sequence at the site.

One important application of genome-editing technology is disease modeling (Musunuru, 2013). The ability to generate isogenic wild-type and mutant clones for phenotypic comparison would enable rigorous functional genetic studies. However, both CRISPR-Cas9 and TALENs have been demonstrated to produce off-target effects, i.e., mutagenesis at sites in the genome other than the desired on-target site (Hockemeyer et al., 2011; Mussolino et al., 2011; Fu et al., 2013; Hsu et al., 2013; Mali et al., 2013a; Pattanayak et al., 2013; Cradick et al., 2013; Cho et al., 2014). These studies have largely focused on sites with high sequence similarity to the on-target site and have documented mutagenesis rates as high as 77% for CRISPR-Cas9 and 1% for TALENs at individual off-target sites. Relatively unexplored is whether CRISPR-Cas9 or TALENs produce off-target effects at sites with low sequence similarity to the on-target site. Although the nucleases might have poor affinity and have a low probability of generating a mutation at any given single site in the genome, they might nonetheless generate a sizeable number of nonspecific mutations across the billions of basepairs of the genome in any single cell. This would significantly confound the validity of disease-modeling studies that rely upon genome-edited clones.

To date, most studies of nuclease off-target effects have been performed in aggregated pools of transformed or immortalized cultured human cells, such as HEK 293T and K562 cells, that are not well suited for disease modeling. We therefore decided to study nuclease off-target effects generated in a "real-world" application of genome editing, centered on human pluripotent stem cell (hPSC) clones being actively used for biological studies (e.g., Ding et al., 2013a).

We assessed the degree of genome-wide off-target mutagenesis in hPSC clones targeted with either CRISPR-Cas9 or TALENs. We performed whole-genome sequencing at high coverage

(60× target coverage) of ten cell lines, including nine clones we had previously generated with genome editing (Ding et al., 2013a; Ding et al., 2013b) (Figure 1): the human embryonic stem cell line HUES 9; three HUES 9 clones exposed to TALENs targeting the *SORT1* gene, with one clone remaining wild-type in both alleles (clone A) and two clones bearing indels in both *SORT1* alleles (clones B and C); three HUES 9 clones exposed to CRISPR-Cas9 targeting the same site in the *SORT1* gene, with one wild-type clone (clone D) and two clones bearing indels in both *SORT1* alleles (clones E and F); and three HUES 9 clones exposed to CRISPR-Cas9 targeting the *LINC00116* gene, with one wild-type clone (clone G) and two clones bearing indels in both *LINC00116* alleles (clones H and I). All of the HUES 9 clones were derived from the same stock of parental HUES 9 cells. Of note, we had found the targeting efficiency of the *SORT1* TALENs to be 11%, in contrast to CRISPR-Cas9 for *SORT1*, which was 76%; the targeting efficiency of CRISPR-Cas9 for *LINC00116* was 57% (Ding et al., 2013b).

Upon obtaining the whole-genome sequencing data, we assessed the clones for small indels, single nucleotide variants (SNVs), and structural variants (SVs), which include chromosomal inversions, rearrangements, duplications, and deletions (Supplemental Experimental Procedures). We largely focused on the identification of small indels and SVs because they comprise virtually all of the mutations introduced by NHEJ. After filtering for the small indels most likely to be true positives and to be potential off-target mutations (rather than mutations that arose in the parental cell pool) and confirmation with Sanger sequencing, we identified a total of 28 such indels across the nine experimental clones, compared against the parental HUES 9 cells as the reference. Of note, all of the previously known on-target indels (seven in total) were correctly identified by the whole-genome sequencing and filtering (Table 1 and Table S1). One of the 28 off-target indels was a frameshift in the coding sequence of *ZDHHC11* (in clone I). None of the other indels lay in either the coding sequence of a gene or the expressed sequence of an annotated non-coding RNA.

None of the indels in CRISPR-Cas9 clones were within 100 nucleotides of a potential off-target site as predicted by sequence similarity—up to six mismatches—with the on-target site, and none lay near sequences that matched the on-target sites better than would be expected by chance (Figure S1). Moreover, none of the indels lay within 100 nucleotides of a sequence perfectly matching the last ten nucleotides of the protospacer with an adjacent PAM site [NGG as well as NAG, which has also been shown to be tolerated (Hsu et al., 2013; Pattanayak et al., 2013)]. Furthermore, we paid special attention to the indels that lay within five bases upstream of a potential PAM site (Table S1), where CRISPR-Cas9-mediated DSBs would be expected to occur. Although the majority of clones had a potential PAM site, none of the adjacent sequences matched the on-target site better than would be expected by chance (Figure S1).

One of the indels in a TALEN clone was located between two potential off-target binding sites as predicted by sequence similarity with the on-target sites—one with three mismatches, and the other with four mismatches—with the binding sites being 17 bp apart, within the optimal range for generating a DSB with TALENs of this type (Ding et al., 2013a) (Figure 1A). None of the other TALEN clone indels were optimally positioned near a pair of degenerate TALEN binding sites (up to five mismatches with the on-target site), and none lay near sequences that matched the on-target sites better than would be expected by chance (Figure S1).

None of the SVs and SNVs that passed our filtering criteria in CRISPR-Cas9 clones was within 100 nucleotides of a predicted off-target site. None of the variants in TALEN clones were optimally positioned near a pair of degenerate TALEN binding sites. We detected 894 unique SNVs across the nine clones (average of 100 per clone) compared to the parental HUES 9 cell line (Table 1). The SV analysis revealed two structural variants unique to an individual clone: a 5.5-kb deletion on chromosome 6 in clone F and a 261-bp segment of chromosome 4 inserted within the *LINC00116* CRISPR-Cas9 on-target site on chromosome 2 in clone H (Table 1 and Table S2). Sanger sequencing confirmed that both alleles of the chromosome 4 region were

intact in clone H, signifying a duplicated insertion into the chromosome 2 on-target site rather than a balanced translocation. We speculate that due to microhomology, the chromosome 4 region was used as a repair template for a DSB at the on-target site.

Just one of the detected variants—a TALEN clone indel—seems certain to be a nuclease-mediated off-target effect. It is probable that some if not all of the other indels/SVs reflect clonal heterogeneity within the original stock of HUES 9 cells. Previous studies have documented mutagenesis occurring during the derivation and expansion of hPSCs (Hussein et al., 2011; Gore et al., 2011; Howden et al., 2011; Yusa et al., 2011). Furthermore, each clone harbored a sizable number of unique SNVs, which would not be predicted to result from NHEJ. Nonetheless, with a maximum of just two to five confirmed events in each individual clone, our results suggest that nuclease-mediated off-target effects of CRISPR-Cas9 and TALENs do not intrinsically cause a large degree of indiscriminate, nonspecific mutagenesis across the genome.

We note the limitations of this study. Even with whole-genome sequencing at high coverage, it is likely that some variants in the clones were not detected given the limitations of short-read sequencing. The small number of sequenced clones targeted at just two loci prevents generalization to all hPSC clones targeted with any CRISPR-Cas9 or TALENs of any configuration by any methodology. Furthermore, our results are not relevant to therapeutic applications targeting up to millions of cells at a time, where rare events may have deleterious consequences.

We do note that clonal heterogeneity may represent a more serious obstacle to the generation of truly isogenic cell lines than nuclease-mediated off-target effects, since each of our clones harbored a very small number of unique indels and SVs (two to five) compared to a relatively larger number of unique SNVs (average of 100) that likely arose spontaneously in culture. This suggests that even if one had in hand a genome-editing tool with perfect specificity, targeted

clones would still be likely to harbor some differences elsewhere in the genome. Rigorous studies will require whole-genome sequencing of the clones used for experiments to fully characterize their mutational profiles, or they will need to include multiple clones for each experimental condition to ensure that potential confounding by any single off-target mutation in a clone is minimized.

ACKNOWLEDGMENTS

This work was supported in part by the Harvard Presidential Scholars Fund of the Harvard Medical School MD/PhD Program (A.V.); grants R00-HL098364 (K.M.), R01-HL118744 (K.M.), R01-DK097768 (K.M.), and R00-MH095867 (M.E.T.) from the United States National Institutes of Health (NIH); the Harvard Stem Cell Institute (K.M.); and Harvard University (Q.D., K.M.). We thank Vamsee Pillalamarri, Carrie Hanscom, and the staffs of the MGH Genomics and Technology Core and NextGen Sequencing Core for technical assistance.

REFERENCES

Cho, S.W, Kim, S., Kim, Y., Kweon, J., Kim, H.S., Bae, S., and Kim, J.S. (2014). Analysis of off-target effects of CRISPR/Cas-derived RNA-guided endonucleases and nickases. Genome Res. *24*, 132–141.

Cho, S.W., Kim, S., Kim, J.M., and Kim, J.S. (2013). Targeted genome engineering in human cells with the Cas9 RNA-guided endonuclease. Nat. Biotechnol. *31*, 230–232.

Cong, L., Ran, F.A., Cox, D., Lin, S., Barretto, R., Habib, N., Hsu, P.D., Wu, X., Jiang, W., Marraffini, L.A., et al. (2013). Multiplex genome engineering using CRISPR/Cas systems. Science *339*, 819–823.

Cradick, T.J., Fine, E.J., Antico, C.J., and Bao, G. CRISPR/Cas9 systems targeting β-globin and CCR5 genes have substantial off-target activity. Nucleic Acids Res. *41*, 9584–9592.

Ding, Q., Lee, Y.K., Schaefer, E.A., Peters, D.T., Veres, A., Kim, K., Kuperwasser, N., Motola, D.L., Meissner, T.B., Hendriks, W.T., et al. (2013a). A TALEN genome-editing system for generating human stem cell-based disease models. Cell Stem Cell *12*, 238–251.

Ding, Q., Regan, S.N., Xia, Y., Oostrom, L.A., Cowan, C.A., and Musunuru, K. (2013b). Enhanced efficiency of human pluripotent stem cell genome editing through replacing TALENs with CRISPRs. Cell Stem Cell *12*, 393–394.

Fu, Y., Foden, J.A., Khayter, C., Maeder, M.L., Reyon, D., Joung, J.K., and Sander, J.D. (2013). High-frequency off-target mutagenesis induced by CRISPR-Cas nucleases in human cells. Nat. Biotechnol. *31*, 822–826.

Gore, A., Li, Z., Fung, H.L., Young, J.E., Agarwal, S., Antosiewicz-Bourget, J., Canto, I., Giorgetti, A., Israel, M.A., Kiskinis, E., et al. (2011). Somatic coding mutations in human induced pluripotent stem cells. Nature *471*, 63–67.

Hockemeyer, D., Wang, H., Kiani, S., Lai, C.S., Gao, Q., Cassady, J.P., Cost, G.J., Zhang, L., Santiago, Y., Miller, J.C., et al. (2011). Genetic engineering of human pluripotent cells using TALE nucleases. Nat. Biotechnol. *29*, 731–734.

Howden, S.E., Gore, A., Li, Z., Fung, H.L., Nisler, B.S., Nie, J., Chen, G., McIntosh, B.E., Gulbranson, D.R., Diol, N.R., et al. (2011). Genetic correction and analysis of induced pluripotent stem cells from a patient with gyrate atrophy. Proc. Natl. Acad. Sci. U. S. A. *108*, 6537–6542.

Hsu, P.D., Scott, D.A., Weinstein, J.A., Ran, F.A., Konermann, S., Agarwala, V., Li, Y., Fine, E.J., Wu, X., Shalem, O., et al. (2013). DNA targeting specificity of RNA-guided Cas9 nucleases. Nat. Biotechnol. *31*, 827–832.

Hussein, S.M., Batada, N.N., Vuoristo, S., Ching, R.W., Autio, R., Närvä, E., Ng, S., Sourour, M., Hämäläinen, R., Olsson, C., et al. (2011). Copy number variation and selection during reprogramming to pluripotency. Nature *471*, 58–62.

Jinek, M., Chylinski, K., Fonfara, I., Hauer, M., Doudna, J.A., and Charpentier, E. (2012). A programmable dual-RNA-guided DNA endonuclease in adaptive bacterial immunity. Science *337*, 816–821.

Jinek, M., East, A., Cheng, A., Lin, S., Ma, E., and Doudna, J. (2013). RNA-programmed genome editing in human cells. Elife *2*, e00471.

Mali, P., Aach, J., Stranges, P.B., Esvelt, K.M., Moosburner, M., Kosuri, S., Yang, L., and Church, G.M. (2013a). CAS9 transcriptional activators for target specificity screening and paired nickases for cooperative genome engineering. Nat. Biotechnol. *31*, 833–838.

Mali, P., Yang, L., Esvelt, K.M., Aach, J., Guell, M., DiCarlo, J.E., Norville, J.E., and Church, G.M. (2013b). RNA-guided human genome engineering via Cas9. Science *339*, 823–826.

Miller, J.C., Tan, S., Qiao, G., Barlow, K.A., Wang, J., Xia, D.F., Meng, X., Paschon, D.E., Leung, E., Hinkley, S.J., et al. (2011). A TALE nuclease architecture for efficient genome editing. Nat. Biotechnol. *29*, 143–148.

Mussolino, C., Morbitzer, R., Lütge, F., Dannemann, N., Lahaye, T., and Cathomen, T. (2011). A novel TALE nuclease scaffold enables high genome editing activity in combination with low toxicity. Nucleic Acids Res. 39, 9283–9293.

Musunuru, K. (2013). Genome editing of human pluripotent stem cells to generate human cellular disease models. Dis. Model. Mech. *6*, 896–904.

Pattanayak, V., Lin, S., Guilinger, J.P., Ma, E., Doudna, J.A., and Liu, D.R. (2013). High-throughput profiling of off-target DNA cleavage reveals RNA-programmed Cas9 nuclease specificity. Nat. Biotechnol. *31*, 839–843.

Yusa, K., Rashid, S.T., Strick-Marchand, H., Varela, I., Liu, P.Q., Paschon, D.E., Miranda, E., Ordóñez, A., Hannan, N.R., Rouhani, F.J., et al. (2011). Targeted gene correction of α1-antitrypsin deficiency in induced pluripotent stem cells. Nature *478*, 391–394.

FIGURE LEGENDS

Figure 1. On-target and Off-target Mutations

(A) HUES 9 clones targeted in the *SORT1* gene with TALENs or CRISPR-Cas9.

(B) HUES 9 clones targeted in the *LINC00116* gene with CRISPR-Cas9. For TALEN targeted clones, the boxes indicate the TALEN on-target and off-target binding sequences. For CRISPR-Cas9 targeted clones, the boxes indicate the 20-bp sequence matching the protospacer and the 3-bp PAM. For the on-target sites, deletions and insertions in the two alleles of each clone are indicated. For the off-target site, the mismatches with the TALEN on-target binding sequences are indicated in bold, and the deletion in one allele of the clone is indicated.

Figure 1

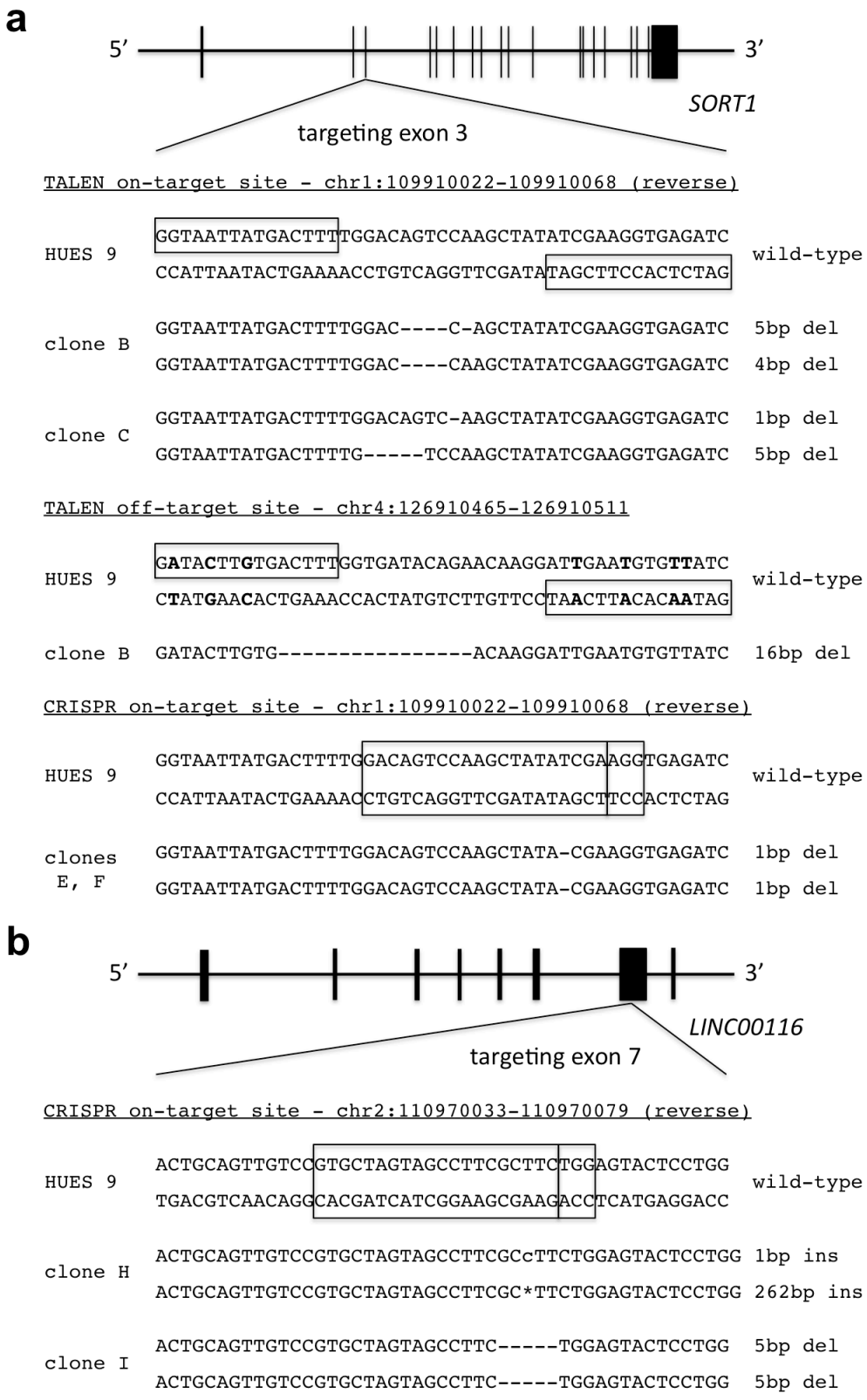
a
5'
3'
SORT1
targeting exon 3
TALEN on-target site - chr1:109910022-109910068 (reverse)
HUES 9
GGTAATTATGACTTTTGGACAGTCCAAGCTATATCGAAGGTGAGATC
CCATTAATACTGAAAACCTGTCAGGTTCGATATAGCTTCCACTCTAG
wild-type
clone B
GGTAATTATGACTTTTGGAC----C-AGCTATATCGAAGGTGAGATC 5bp del
GGTAATTATGACTTTTGGAC----CAAGCTATATCGAAGGTGAGATC 4bp del
clone C
GGTAATTATGACTTTTGGACAGTC-AAGCTATATCGAAGGTGAGATC 1bp del
GGTAATTATGACTTTTG-----TCCAAGCTATATCGAAGGTGAGATC 5bp del
TALEN off-target site - chr4:126910465-126910511
HUES 9
GATACTTGTGACTTTGGTGATACAGAACAAGGATTGAATGTGTTATC
CTATGAACACTGAAACCACTATGTCTTGTTCCTAACTTACACAATAG
wild-type
clone B GATACTTGTG----------ACAAGGATTGAATGTGTTATC 16bp del
CRISPR on-target site - chr1:109910022-109910068 (reverse)
HUES 9
GGTAATTATGACTTTTGGACAGTCCAAGCTATATCGAAGGTGAGATC
CCATTAATACTGAAAACCTGTCAGGTTCGATATAGCTTCCACTCTAG
wild-type
clones E, F
GGTAATTATGACTTTTGGACAGTCCAAGCTATA-CGAAGGTGAGATC 1bp del
GGTAATTATGACTTTTGGACAGTCCAAGCTATA-CGAAGGTGAGATC 1bp del
b
5'
3'
LINC00116
targeting exon 7
CRISPR on-target site - chr2:110970033-110970079 (reverse)
HUES 9
ACTGCAGTTGTCCGTGCTAGTAGCCTTCGCTTCTGGAGTACTCCTGG
TGACGTCAACAGGCACGATCATCGGAAGCGAAGACCTCATGAGGACC
wild-type
clone H
ACTGCAGTTGTCCGTGCTAGTAGCCTTCGCcTTCTGGAGTACTCCTGG 1bp ins
ACTGCAGTTGTCCGTGCTAGTAGCCTTCGC*TTCTGGAGTACTCCTGG 262bp ins
clone I
ACTGCAGTTGTCCGTGCTAGTAGCCTTC-----TGGAGTACTCCTGG 5bp del
ACTGCAGTTGTCCGTGCTAGTAGCCTTC-----TGGAGTACTCCTGG 5bp del

Table 1. Numbers of Unique On-target and Candidate Off-target Indels and Structural Variants (SVs), As Well As Unique Single Nucleotide Variants (SNVs), in TALEN and CRISPR-Cas9 Targeted Clones

	SORT1 TALENs			*SORT1* CRISPR-Cas9			*LINC00116* CRISPR-Cas9		
clones	A	B	C	D	E	F	G	H	I
on-target indels	—	2	2	—	1[a]	1[a]	—	1	1[a]
on-target SVs	—	—	—	—	—	—	—	1[b]	—
likely off-target indel	—	1	—	—	—	—	—	—	—
other candidate off-target indels	2	1	2	4	4	2	3	5	4
candidate off-target SVs	—	—	—	—	—	1	—	—	—
SNVs	64	115	142	55	94	74	111	127	112

See also Figure S1 and Tables S1–S3.

[a] Homozygous for indels.

[b] 261 bp duplicated insertion.

SUPPLEMENTAL DATA

Figure S1, Related to Table 1. Minimal Edit Distances Near Indels

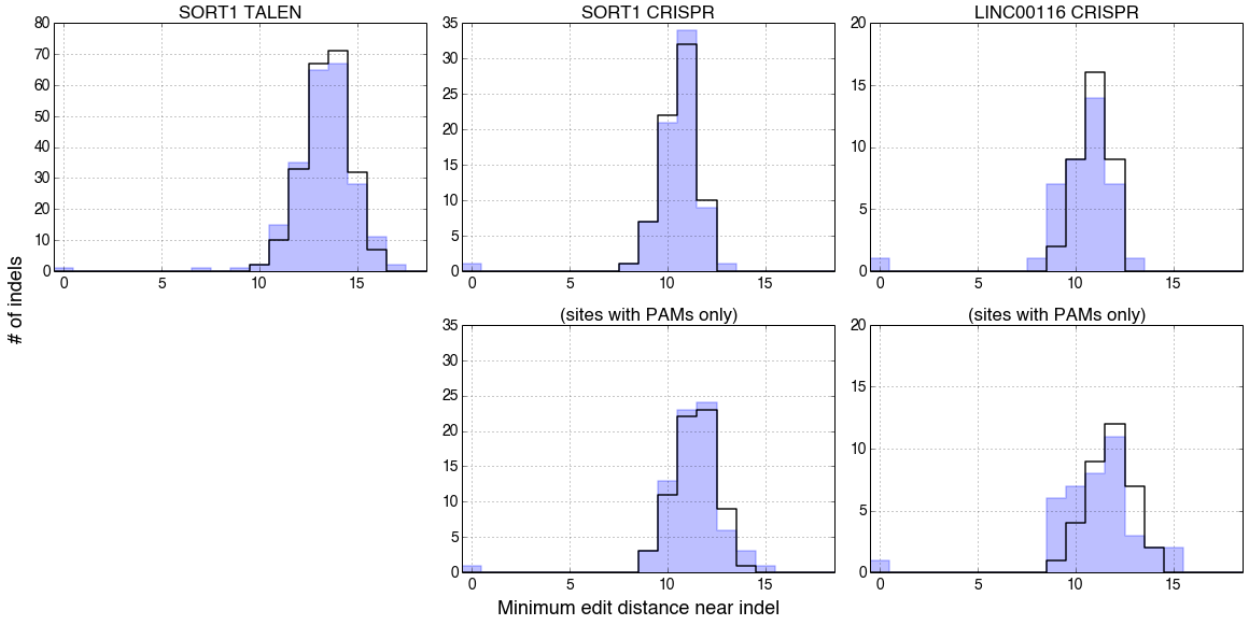

In each panel, the blue shaded area represents the distribution of minimal edit distances for each nuclease's subset of 381 filtered indels, and the black line represents the expected distribution inferred from 50,000 randomly sampled parental HUES 9 line indels. Top row, minimal edit distances across a 100-bp window around a given indel. Bottom row, minimal edit distances across a 100-bp window, retaining only sequences that end in an NGG or NAG PAM sequence.

Table S1, Related to Table 1. Unique Indels Detected by Whole-genome Sequencing

						SORT1 TALENs			*SORT1* CRISPR-Cas9			*LINC00116* CRISPR-Cas9		
Chr	Pos	5' flanking sequence	Ref	Alternate	3' flanking sequence	A	B	C	D	E	F	G	H	I
1	81390259	ATAGCCTAAGAAGATATTCC	CATATGGTG	C	TTCTCAGAGCTCTTAGTGTG									25,11
1	**109910034**	**GTGTTATTGATCTCACCTTC**	**G**	**GA**	**ATATAGCTTGGACTGTCCAA**					**0,13**	**1,54**			
1	**109910041**	**GATCTCACCTTCGATATAGC**	**TTGGACT**	**TG**	**GTCCAAAAGTCATAATTACC**		**9,4***							
1	**109910043**	**ATCTCACCTTCGATATAGCT**	**TG**	**T**	**GACTGTCCAAAAGTCATAAT**			**7,17***						
1	**109910044**	**TCTCACCTTCGATATAGCTT**	**GGACT**	**G**	**GTCCAAAAGTCATAATTACC**		**5,8***							
1	**109910046**	**TCACCTTCGATATAGCTTGG**	**ACTGTC**	**A**	**CAAAAGTCATAATTACCAGT**			**20,8***						
1	170931870	AATTTGTGCCTAATTTGAGC	TG	T	TTTTTTTTAATTCATTTAAA					8,17				
2	9705788	CGAGAGACTGAAAGAAAAGC	AGCAAAGCCCTGGGT	A	AATCAAGGCCCTAAACGGAA		8,5							
2	76409962	ACAAGTTGAAGATGACAATC	TG	T	TGGCAATTCTACAATATTGT				14,7					
2	**110970046**	**TGCCAGCCCAGGAGTACTCC**	**AGAAGC**	**A**	**GAAGGCTACTAGCACGGACA**									**4,58**
2	**110970049**	**CAGCCCAGGAGTACTCCAGA**	**A**	**AG**	**GCGAAGGCTACTAGCACGGA**								**1,34**	
2	136347377	GACTTGGATAATATATCTGT	CACATTATATAATATATATTATGC AAATCTGTT	C	ACATTATATAATATATATGA			12,10						
3	138374851	TATGTACTTCCCAGATTCTT	TC	T	CCTCCTGGCTAAGAACCATC				16,11					
3	195706577	CCACACGCTTACAAGACACA	C	CAT	GAGCCGAACGCTTTCCGGGC						5,3			
4	65647862	TATTAGTAAGCAAAACATGC	TG	T	TTTGAGTAGTTATGATTTTG	11,12								
4	67241317	TGACAATCATAACTTTTTTA	G	GCCT	CCTCTATGCACACAGAAAAG			11,10						
4	117364346	TTTAAAATATTATCTATGAG	GAATATTTTC	G	TATATTTTTACCTTGAATAT						9,5			
4	**126910474**	**TTCACAGGAAAGATACTTGT**	**GACTTTGGTGATACAGA**	**G**	**ACAAGGATTGAATGTGTTAT**		**8,4**							
5	**850612**	**CTGGAAGTAGTGCAGGGGTA**	**AC**	**A**	**GACCAGCCGTTCACTCTGGA**									**43,15**
5	32712655	CCAGGCCAGTGAGAGAGGTG	A	AG	GCAGGGGCGCGTCCCGGGCC								30,35	
6	156267271	TTTAAAGCCATGTGTTTTAG	TA	T	ACTAAATGTTGCTGCTTTAG					13,12				
7	23212217	GTGTGAAGAAAGAAAAAAGA	ATTAT	A	TTATCTTCGAAGCATCTTCC					19,16				
8	127961691	ATTGATTTGCTATGGGCAAA	A	AAG	AAAAAAAAAAAAAAGAGGAA				4,5					
8	132181273	AAATCCCTTCAAATTTTGTT	TCTAC	TGAAGGGATTTA	ATTTTCTAAACCTAATATTG								6,11	
9	33682336	TGAGTCTTGGAAACATTTGT	GAA	G	ATTCTTATTCTGAGTTTGCC	18,14								
10	30327724	ATACAAATGAAGGAAGAAGG	G	GTA	TATAGGTCCATGTGGAAGGA							34,7		
10	82813787	TAGAAAAGCAGAAAGACTGA	GTCTC	G	TATGAGAGATGTGTTATCGT								18,25	
10	131460181	TGCTACACCCTTTCCATAGG	CT	C	TCACTGTCATCTACCCTCAT								33,8	
11	85267884	CCTCATACAAAGTTTATTCT	CTCT	C	TCTAGTTATCCAAATATAGA								13,15	
12	30161597	TTGTGGAGTCCACCTCATGA	CCTTGTATGGACAGATAGACAT	C	CTAACCTGTTCTTGTGAACT				34,12					
13	71581221	AAAAACACTATGAATTCACA	CATATTTT	C	ATATCTGAAAACATTACCAT							11,3		
14	68143591	AAAAAATAATCAAAAAGAAT	TTTTA	T	TTTGTCATTGACAGTTCAAT					12,6				
17	5015438	GCGGGTGACTTCATCAAGTT	TG	T	GGGGGTCTCTTGTGGAATTG									29,11
18	39827854	CTTGTGATGACAGCAACCAC	C	CAAAT	AAATAACTTGATAGAATTTT							21,6		
22	28415750	TTCGCCCTGGCTGACTTCTC	TTTGCC	T	TCAGCTCTCTGGGCTCTAGA									50,35

Indels at on-target sites are indicated in red bold. A likely nuclease-mediated off-target indel is indicated in blue bold. An indel that lies in the coding sequence of *ZDHHC11* is indicated in magenta bold. Underlines indicate potential PAMs (NGG or NAG) within five bases upstream of the indel. Columns A–I indicate reference allele counts (x) and alternate allele counts (y) in the format (x,y) for any of the clones A–I in which the called genotype included at least one copy of the alternate allele. Note: the reference allele counts for the on-target indels in clones B and C marked in red bold and with (*) do **not** indicate wild-type alleles—rather, due to the nature of the calling algorithm, they indicate counts of alleles that do not match the alternate alleles; because clones B and C are compound heterozygotes, the reference allele counts actually represent the indels on the other alleles. All on-target and off-target indels in this Table were confirmed with Sanger sequencing.

Table S2, Related to Table 1. Unique Structural Variants (SVs) Detected by Whole-genome Sequencing

SV class	Clone	Treatment group	Chr	Start	End	Size	Split-read consensus
Translocation[a]	**H**	***LINC00116* CRISPR-Cas9**	**4**	**183998625**	**183998885**	**261 bp**	**chr2 | chr4: CTGCCAGCCCAGGAGTACTCCAGAA | G | CTTACATTTGGGGTTGTGATTCTGG** **chr4 | chr2: CTGGAGGATCCCTTGAGCACAGGAGT | GCGAAGGCTACTAGCACGGACAACT**
Deletion[b]	F	*SORT1* CRISPR-Cas9	6	18754456	18760023	5568 bp	N/A

A structural variant at an on-target site is indicated in red bold. Split-read consensus sequences represent the consensus of all split reads that span the breakpoint. Vertical lines denote precise breakpoint positions.

[a] Translocation represents a duplicated insertion from chromosome 4 that inserted into the on-target chromosome 2 site. The underlined base in the split-read consensus indicates an additional inserted basepair at the breakpoint.

[b] As no split-reads spanned this event, there is not precise refinement of the coordinates.

Table S3, Related to Table 1. Numbers of Indels and Single Nucleotide Variants (SNVs) Detected by Whole-genome Sequencing

		HUES 9	A	B	C	D	E	F	G	H	I
Raw indel calls	Total	881063	879305	878638	886519	867987	889297	873304	874320	875199	873847
	Missed[a]		39191	43335	43159	35729	43211	36810	36181	35699	34666
	De novo		40949	45760	37703	48805	34977	44569	42924	41563	41882
Post low-complexity filter	Total	198172	198325	198116	198923	197398	199108	197898	197542	197589	197436
	Missed[a]		3518	4051	3910	3198	3953	3325	3006	2968	2885
	De novo		3365	4107	3159	3972	3017	3599	3636	3551	3621
Post homopolymeric filter	Total	119573	119899	119710	119980	119555	120026	119735	119486	119563	119513
	Missed[a]		1220	1457	1334	1007	1359	1074	881	878	852
	De novo		894	1320	927	1025	906	912	968	888	912
De novo, nuclease-specific indels			69	195	146	25	57	30	22	20	17
Sample-specific indels			8	78	39	9	29	9	13	12	13
Called reads in only one sample, > 2 reads[b]			3	10	10	4	6	2	3	6	7
Confirmed by Sanger sequencing			2	4	4	4	4	2	3	6	5
		HUES 9	A	B	C	D	E	F	G	H	I
Raw SNV calls	Total	3698888	3707753	3705830	3714888	3695767	3713222	3704487	3695231	3697396	3697034
	Missed[a]		35795	47106	45002	28291	40247	33049	25713	26172	26165
	De novo		26930	40164	29002	31412	25913	27450	29370	27664	28019
Post low-complexity filter	Total	1531069	1533920	1531422	1534449	1531074	1534452	1533074	1530709	1531112	1530978
	Missed[a]		7984	9645	9401	6064	8694	7238	5313	5349	5280
	De novo		5133	9292	6021	6059	5311	5233	5673	5306	5371
De novo, nuclease-specific SNVs			670	1593	1513	195	472	344	235	269	206
Sample-specific SNVs			165	595	538	110	269	163	159	192	147
Called reads in only one sample, > 2 reads			64	115	142	55	94	74	111	127	112

[a] Calls in the parental HUES 9 line that were not called in the individual clone.

[b] Not included in this tally is an on-target indel shared by clones E and F.

SUPPLEMENTAL EXPERIMENTAL PROCEDURES

Generation of TALEN targeted and CRISPR-Cas9 targeted clones

The targeted clones were generated as previously described (Ding et al., 2013a; Ding et al., 2013b; Peters et al., 2013). We summarize the methods below. The CRISPR-Cas9 and TALENs used were chosen for the proximity of their predicted binding sites to the desired target sites in the genes, and the TALENs were designed as an obligate heterodimer. For each CRISPR-Cas9, there were no sequences elsewhere in the genome with up to two mismatches with the 20-nucleotide target site.

TALEN genomic binding sites in *SORT1* were chosen to be 15 bp in length such that the target sequence between the two binding sites was between 14 and 18 bp in length; each binding site was anchored by a preceding T base in position "0" as has been shown to be optimal for naturally occurring TAL proteins. We generated full-length TALENs harboring, in order: a N-terminal FLAG tag, a nuclear localization signal, the N-terminal portion of the TALE PthXo1 from the rice pathogen *X. oryzae* pv. oryzae lacking the first 176 amino acids, the engineered TAL repeat array, the following 63 amino acids from the corresponding C-terminal portion of PthXo1 and one of two enhanced FokI domains. The FokI domains used were obligate heterodimers with both the Sharkey and ELD:KKR mutations to enhance cleavage activity, engineered by PCR. Each TALEN was in a plasmid with the CAG promoter for optimal expression in human pluripotent stem cells, with the TALEN being coexpressed with a fluorescent marker [enhanced green fluorescent protein (EGFP), mCherry (Clontech), or turbo red fluorescent protein (tRFP; Evrogen)] via an intervening viral 2A sequence. For CRISPR-Cas9, we subcloned a human codon-optimized Cas9 gene with a C-terminal nuclear localization signal into the same CAG expression plasmid with EGFP, and we separately expressed the guide

RNA (gRNA) from a plasmid with the human U6 polymerase III promoter. The 20-nucleotide protospacer sequence for each gRNA was introduced using polymerase chain reaction (PCR)-based methods. The reagents used to generate these various TALEN and CRISPR-Cas9 plasmids are available through Addgene (https://www.addgene.org/talen/musunuru/ and https://www.addgene.org/crispr/musunuru/).

HUES 9 cells were grown in feeder-free adherent culture in chemically defined mTeSR1 (STEMCELL Technologies) supplemented with penicillin/streptomycin on plates pre-coated with Geltrex matrix (Invitrogen). The cells were disassociated into single cells with Accutase (Invitrogen), and 10 million cells were electroporated with 50 μg of the TALEN pair (25 μg of each plasmid) or CRISPR-Cas9 (25 μg of each plasmid) in a single cuvette and replated. The cells were collected from the culture plates 48 to 72 hours post-transfection or post-electroporation (at which point fluorescent marker expression was in decline) by Accutase treatment and resuspended in PBS. Cells expressing green and/or red fluorescent markers were collected by FACS (FACSAria II; BD Biosciences) and replated on 10-cm tissue culture plates at 15,000 cells/plate to allow for recovery in growth media.

Post-FACS, the cells were allowed to recover for 7-10 days, after which single colonies were manually picked and dispersed and replated individually to wells of 96-well plates. Colonies were allowed to grow to near confluence over the next 7 days, at which point they were split using Accutase and replica-plated to create a working stock and a frozen stock. The working stock was grown to confluence, and genomic DNA was extracted in 96-well format, followed by PCR amplification around the target site and Sanger sequencing to identify both untargeted and targeted clones. Chosen clones were expanded further for extraction of genomic DNA for whole-genome sequencing, with ~7 passages occurring between the single-cell cloning and the DNA extraction.

Identification of novel indels, single nucleotide variants, and structural variants

Genomic DNA from all ten cell lines (parental HUES 9 line, clones A–I) was extracted using the DNeasy Tissue Kit (QIAGEN) and subjected to quality assessment. The extracted DNA was sequenced as paired-end 101-nucleotide reads to a target of 60× haploid coverage on an Illumina HiSeq2000 sequencer as previously described (Stransky et al., 2011). These mate-pair libraries featured an average median fragment insert size of 329 bp and a standard deviation of 47 bp. The pair-ends reads were aligned onto the *hg19* (GRCh37v. 71) human reference genome using Bowtie 2 and manipulated (deduplication, sorting, indexing) using Picard Tools, version 1.84 (http://picard.sourceforge.net). The reads have been uploaded to the NCBI Short Read Archive (SRA) and are available via the accession number SRP039576.

The Genome Analysis ToolKit, version 2.6 (McKenna et al., 2010), was used for local realignment around indels (RealignerTargetCreator, IndelRealigner), base score recalibration (BaseRecalibrator), variant calling across the ten samples (HaplotypeCaller) and variant score recalibration (VariantRecalibrator, ApplyRecalibration). Candidate indels (totalling 948,344 calls) were filtered on several criteria using Python and the PyVCF, version 0.6.0, and PyFasta, version 0.5.0, packages. First, we removed indels near low-complexity regions as defined by RepeatMasker and annotated by softmasking in hg19). Indels were considered "near" low complexity regions if any position within 10 bp or at least one third of positions within 50 bp were masked by RepeatMasker. Second, we removed indels that caused expansions or compressions of long (>6 bp) homopolymers. The effects of these filters are detailed in Table S3. By comparing indels calls in the parental HUES 9 cell line to calls for each of the clones, we can estimate false-negative rates of 4%-6% (in raw indel calls) and ~1% (after these two filters). Considering only indels that (1) were absent in the parental HUES 9 cell line and (2) were not called in samples that were treated with different nucleases (TALENs for *SORT1*, CRISPR-Cas9 for *SORT1*, CRISPR-Cas9 for *LINC00116*), we produced a set of 381 indels used in further

analyses. Among these 381 indels were seven on-target indels already known to be in the targeted clones via Sanger sequencing (Table S1).

We further filtered the 381 indels to identify those most likely to represent nuclease-mediated off-target effects by: (1) retaining indels for which there were called alternate alleles in only one sample, since indels generated by engineered nucleases at a given locus are extremely heterogeneous with respect to length and sequence, and it is unlikely that two independent clones would have suffered exactly the same indel at the same off-target site; and (2) retaining indels with the alternate allele present in more than two reads. This yielded a total of 53 indels. We then performed polymerase chain reaction (PCR) amplification and Sanger sequencing to confirm or refute these indels. This yielded a final list of 35 indels, including the seven on-target alleles (Table S1). Thus, at this final stage the false positive rate was 34%.

We searched the human genome for sites likely to exhibit off-target activity based on similarity to nuclease target sites. For CRISPR-Cas9, we considered two types of similar sequences: (1) any sequence within 6 (or fewer) substitutions of the 20-nt target site followed by an NRG PAM sequence and (2) any sequence matching the last 10 nt of the target site follow by an NRG PAM. Using Bowtie 1, we mapped these sequences to 14,200 and 10,935 loci of high similarity relative to the on-target *SORT1* and *LINC00116* sequences. Of note, by intentional design of the CRISPR-Cas9 on-target sites, there were no loci within 2 substitutions of the 20-nt target site. Except for the on-target indels, none of these genomic loci were within 100 bp of indels called in the respective samples.

For TALENs, we constructed a list of all sequences within 5 (or fewer) substitutions of either monomer's on-target site and identified 12,301,606 genomic loci matching these sequences. We manually reviewed 142 indels occurring within 100 bp of these loci. We also identified 55,503 pairs of off-target binding sites facing each other (i.e., oriented towards each other on opposite

strands) and separated by a distance of 10-22 bp. Besides the on-target indels, only one indel occurred between the pair's binding sites, likely representing a bona fide off-target effect.

We expanded our search to nearby off-target sites with any possible number of mismatches relative to the target sequences. We searched 100-bp windows around each indel for the sequence most closely matching the on-target site and recorded the number of mismatches of that sequence. We refer to this number as the minimal edit distance of the region near an indel. To prevent double counting, we merged the windows of indels within 100 bp of each other. For CRISPR-Cas9, we allowed for both NGG and NAG PAM sequences when counting mismatches. For TALENs, we considered every pair of sequences in the window regardless of the distance separating them. We computed minimal edit distances for the 381 indels (Figure S1, blue areas) and compared each nuclease's distribution to background distributions determined by the minimal edit distances of 50,000 randomly chosen parental HUES 9 line indels that passed low-complexity and homopolymer filters (Figure S1, black lines). The only outliers we observed were the on-target events (minimal edit distance of 0) and the single TALEN off-target event (minimal edit distance of 7).

Candidate SNVs (totalling 3,776,763 calls) were filtered using criteria similar to the indels (Table S3). We removed SNVs near low-complexity regions and considered only SNVs (1) absent in the parental HUES 9 cell line and (2) not called in samples that were treated with different nucleases. Together, these filters produced a set of 1,742 SNVs. We applied the same final filters described above for indels; this resulted in a final list of 894 SNVs (Table 1). Using the same CRISPR-Cas9 and TALEN off-target analyses described above for indels, we determined that none of the SNVs lay in proximity to predicted off-target sites.

We sought to establish the structural variation (SV) architecture of each individual line and then compared the SV burden across technical approaches and in comparison to the parental HUES 9

line, including inversions, rearrangements, duplications, and deletions. All paired-end data were aligned with BWA-MEM, version 0.7.5a-r418 (Li, 2013), to *GRCh37.71* using defaults with duplicate reads removed using Picard Tools. We used an integrated SV detection pipeline synthesized from four previously published algorithms: LUMPY, version 0.1.5 (Layer et al., 2012), DELLY, version 0.0.11 (Rausch et al., 2012), BAMSTAT, version 0.2 (Talkowski et al., 2011; Talkowski et al., 2012; Chiang et al., 2012), and CNVnator, version 0.2.7 (Abyzov et al., 2011). The principal branch of the pipeline generated a preliminary SV set by intersecting paired-end evidence from DELLY-PE and BAMSTAT with consensus split read call-sets derived from LUMPY-SR and DELLY-SR. These calls were further screened for high-confidence using mapping quality (MapQ $\geq$ 20) and a minimum event size equal to the mean insert size plus six times the insert size standard deviation for each that particular library (ranging from 754 bp to 866 bp; library-dependant).

Following initial filtering, we performed in silico PCR validation of split-reads supporting the event and filtered all SVs against established reference artifacts and unplaced contigs from ongoing studies in our laboratory and others (M. Talkowski, unpublished data). An analogous branch of the SV detection pipeline further supplemented these SV calls with a genome-wide focal read-depth analysis (CNVnator) and ancillary anomalous mate-pair clustering (DELLY-PE) to capture de novo CNVs. We generated a list of candidate CNVs across all libraries that passed CNVnator's hardcoded e-value filter. We further filtered these candidate CNVs for high confidence based on CNV size, normalized read depth, and proportion of reads within the putative CNV with mapping quality $\geq$ 0, as consistent with CNVnator's recommended filtering criteria. Finally, we refined these CNV calls with concordant evidence of anomalous paired-end support from DELLY-PE. As with indels, we focused on SVs and CNVs that were unique to individual clones.

Of note, we identified a pericentric inversion of chromosome 9 [inv(9)(p11.2q13)] in our consensus call set that was consistent with a previously annotated pericentric inv(9) in the HUES 9 cell line, thought to be of no clinical consequence (Feuk, 2010).

SUPPLEMENTAL REFERENCES

Abyzov, A., Urban, A.E., Snyder, M., and Gerstein, M. (2011). CNVnator: an approach to discover, genotype, and characterize typical and atypical CNVs from family and population genome sequencing. Genome Res. *21*, 974–984.

Chiang, C., Jacobsen, J.C., Ernst, C., Hanscom, C., Heilbut, A., Blumenthal, I., Mills, R.E., Kirby, A., Lindgren, A.M., Rudiger, S.R., et al. (2012). Complex reorganization and predominant non-homologous repair following chromosomal breakage in karyotypically balanced germline rearrangements and transgenic integration. Nat. Genet. *44*, 390–397, S1.

Feuk, L. (2010). Inversion variants in the human genome: role in disease and genome architecture. Genome Med. *12*, 11.

Layer, R.M., Hall, I.M., and Quinlan, A.R. (2012). LUMPY: A probabilistic framework for structural variant discovery. arXiv:1210.2342v1 [q-bio.GN].

Li, H. (2013). Aligning sequence reads, clone sequences and assembly contigs with BWA-MEM. arXiv:1303.3997v2 [q-bio.GN].

McKenna, A., Hanna, M., Banks, E., Sivachenko, A., Cibulskis, K., Kernytsky, A., Garimella, K., Altshuler, D., Gabriel, S., Daly, M., et al. (2010). The Genome Analysis Toolkit: a MapReduce framework for analyzing next-generation DNA sequencing data. Genome Res. *20*, 1297–1303.

Peters, D.T., Cowan, C.A., and Musunuru, K. (2013). Genome editing in human pluripotent stem cells. StemBook [Internet]. Cambridge (MA): Harvard Stem Cell Institute; 2008–.

Rausch, T., Zichner, T., Schlattl, A., Stütz, A.M., Benes, V., and Korbel, J.O. (2012). DELLY: structural variant discovery by integrated paired-end and split-read analysis. Bioinformatics *28*, i333–i339.

Stransky, N., Egloff, A.M., Tward, A.D., Kostic, A.D., Cibulskis, K., Sivachenko, A., Kryukov, G.V., Lawrence, M.S., Sougnez, C., McKenna, A., et al. (2011). The mutational landscape of head and neck squamous cell carcinoma. Science *333*, 1157–1160.

Talkowski, M.E., Ernst, C., Heilbut, A., Chiang, C., Hanscom, C., Lindgren, A., Kirby, A., Liu, S., Muddukrishna, B., Ohsumi, T.K., et al. (2011). Next-generation sequencing strategies enable routine detection of balanced chromosome rearrangements for clinical diagnostics and genetic research. Am. J. Hum. Genet. *88*, 469–481.

Talkowski, M.E., Rosenfeld, J.A., Blumenthal, I., Pillalamarri, V., Chiang, C., Heilbut, A., Ernst, C., Hanscom, C., Rossin, E., Lindgren, A.M., et al. (2012). Sequencing chromosomal abnormalities reveals neurodevelopmental loci that confer risk across diagnostic boundaries. Cell *149*, 525–537.